



# Thermal stability and lifetime estimates of a high temperature epoxy by $T_g$ reduction



Benjamin J. Anderson

Material Science and Engineering Center, Sandia National Laboratories, Albuquerque, NM 87185-0958, USA

## ARTICLE INFO

### Article history:

Received 9 May 2013

Received in revised form

15 July 2013

Accepted 2 August 2013

Available online 13 August 2013

### Keywords:

Epoxy

Degradation

Thermal aging

Lifetime

## ABSTRACT

Thermal degradation of a high temperature epoxy network is studied in terms glass transition temperature ( $T_g$ ) reduction over a temperature window encompassing the  $T_g$  of the network. The  $T_g$  is shown to decrease as the network is thermally aged at elevated temperatures in air and in argon. The duration of the aging experiments is extended to long time such that the absolute  $T_g$  reduction approaches a long time reduction plateau. Degradation is dominated by non-oxidative pyrolysis with a small contribution from diffusion limited thermal oxidative degradation at the surface. A time–temperature superposition is constructed from the extent of  $T_g$  reduction of samples aged in air and the thermal shift factors are shown to have Arrhenius scaling behavior. An activation energy is extracted that agrees with previous activation energy measurements derived from other property measurements of the same network aged under similar conditions. The agreement of the activation energy with past results shows that  $T_g$  reduction is controlled by the same degradation mechanism and may be used as an observable for lifetime estimates when thermal degradation is pyrolytic in nature. The extent of  $T_g$  reduction is modeled with an autocatalytic rate expression and compared to previous property measurements to show the difference in sensitivity of observable material properties on degradation.

© 2013 Elsevier Ltd. All rights reserved.

## 1. Introduction

Material lifetimes are the result of aging experiments which study the degradation of materials in time [1–4]. Aging experiments are often conducted on shorter timescales than the required lifetime of a material. Typical aging experiments accelerate the degradation of a material, several hours in a short experiment to days or years in a long experiment. Whereas the duration of an aging experiment tends to be short, the required lifetime of a material in use is usually much longer, several years to decades of years.

Lifetime determined from an aging experiment is based on a measured observable property that is shown to change due to material degradation. The rate of change in the observable is used to quantify a rate of degradation which in turn is used to predict lifetimes in the use environment. Predicted lifetime relies on the determination of a degradation activation energy which quantifies the relationship between temperature and the rate of degradation. The extraction of an activation energy requires that the rate of degradation be proportional to a reaction rate constant that follows an Arrhenius relation,

$$r_d \propto k_d(T) = k_{o,d} e^{-E_a/RT} \quad (1)$$

E-mail address: [bjander@sandia.gov](mailto:bjander@sandia.gov).

where  $r_d$  is the rate of degradation,  $k_d(T)$  is the degradation reaction rate constant,  $k_{o,d}$  is the degradation pre-exponential,  $E_a$  is the activation energy,  $R$  is the gas constant,  $T$  is temperature [2,5]. The mechanism of degradation is assumed to be unchanged over the evaluated temperature range as long as the rate of degradation maintains an exponential inverse temperature dependence with a constant activation energy [1,4]. The activation energy enables the rate of degradation to be predicted as a function of time at a temperature of interest through extrapolation of the Arrhenius temperature dependence. Many studies in the recent years show that material degradation often does not follow an Arrhenius temperature dependence when a large temperature window is sampled during an aging experiment [1,6–8]. The emergence of a new degradation mechanism is identified by a change in the exponential inverse temperature dependence of the rate of degradation. This is commonly shown graphically in an Arrhenius plot by curvature which may signify the presence of many competing degradation mechanisms or a point of discontinuity which signifies a transition to a more energetically favorable degradation mechanism. Since lifetime extrapolations assume that the degradation mechanism remains unchanged, identifying the degradation mechanism and the environmental conditions that lead to the emergence of competing mechanisms is necessary for determining when a lifetime extrapolation and predicted lifetime is anticipated to be valid.

In addition, the smaller the  $\Delta T$  of the extrapolation, the lower the risk of a new degradation mechanism emerging that would cause the true lifetime of a material at the use temperature to differ from the predicted lifetime.

The predicted lifetime from a time–temperature extrapolation is not a true lifetime, but rather a lifetime estimate. The reliability of the estimate depends on whether the observable being measured captures the true failure mode of the material in the use environment. Most observables are not a direct measurement of degradation but a secondary measurement. If the observable is directly impacted by degradation, then the observable may be used as a means to measure the rate of degradation. Lifetime estimates for a material are determined from measurement of the rate of reduction of the measured observable in time (e.g., weight [9], tensile strength [6], elongation [7], adhesion [10], compression relaxation [11], impact strength [12]).

All lifetime estimates are relative to the observable used to determine the lifetime (e.g., weight loss cannot be used to estimate lifetime with respect to adhesion, adhesion loss cannot be used to estimate lifetime with respect to  $T_g$  reduction). Therefore, it is important to select the proper degradation stimulus (e.g., heat, stress, humidity, electrical current, etc.) and observable (e.g., weight, adhesion, electrical breakdown, compression set, modulus,  $T_g$ , etc.) that will be important to function of the material during use. For high temperature use, thermal degradation often poses the greatest risk to reliability; however, the mode by which thermal degradation leads to failure will depend on the application. There is always a question of which observable should be measured to determine the aging performance of a material. Therefore, it is important to understand how degradation can affect different material properties. Understanding the sensitivity of an observable to degradation is a part of aging experiments. This enables a determination of what material properties pose the greatest risk to reliability.

Many commercial high temperature polymers have been developed. Some are used as encapsulants and adhesives for potting and joining. The majority of these high temperature polymers fall into one of six material types: epoxy, phenolic, bismaleimide, cyanate ester, bismaleimide triazine (BT), polyimide. Each material type has advantages and disadvantages compared to the others [13]. Epoxy and cyanate ester tend to have good processability but lower thermal stability, while phenolic, bismaleimide, BT and polyimide tend to have better thermal stability but are more difficult to process. Due to the strenuous environment that high temperature

polymers must survive, it is important to have a good understanding of material lifetime in order to select a reliable polymer.

In a previous paper, thermal degradation of high temperature epoxy cured networks was assessed by loss of adhesive strength [10]. The result was compared to degradation as measured by loss of weight. While the relative time scale of degradation in terms of the measured property differed, the thermal scaling of degradation followed an Arrhenius relation with an activation energy that was the same for both measured properties showing the underlying chemical degradation mechanism is unchanged. However, the time dependence of the extent of degradation was dramatically different between the two measurements even though the activation energies agreed. This result showed that the lifetime estimates of a material depend on the observable being measured (i.e., weight should not be used to estimate the lifetime of an adhesive since bondline failure may occur on a different time scale than weight loss when the same chemical degradation mechanism is affecting both properties). If the wrong failure mode is assumed, a lifetime estimate based on an observable that represents the assumed failure mechanism may under or over predict the material lifetime. It is important when evaluating the lifetime of a material that the aging of a material be studied in a manner that is relevant to the application. It may be unknown which property is more important in gaging material lifetime. Therefore, several properties may need to be studied and the timescales of degradation compared in order to discern a probable mode of failure.

One material property that has received less attention compared to others (e.g., weight loss) as to the influence of degradation is the glass transition temperature,  $T_g$  [14,15]. Above  $T_g$ , polymeric adhesives and encapsulants soften leading to a dramatic change in mechanical performance. Adhesives are known to see a reduction in adhesive and cohesive strength as temperature exceeds the  $T_g$  of the adhesive [16]. Encapsulants soften and could crack in high stress environments. Therefore, an adhesive or encapsulant that is subjected to an environment that causes a reduction in  $T_g$  may see its lifetime severely shortened if the  $T_g$  of the material drifts below the use temperature. If a reduction in  $T_g$  is not appreciated, a lifetime estimate of a material derived from aging experiments may overestimate the lifetime if  $T_g$  reduction occurs at shorter time than the observable used for the lifetime estimate.

In this paper, thermal oxidative degradation of a high temperature epoxy cured network is studied through measurement of  $T_g$ . The  $T_g$  of polymer thermosets is dependent on the crosslink

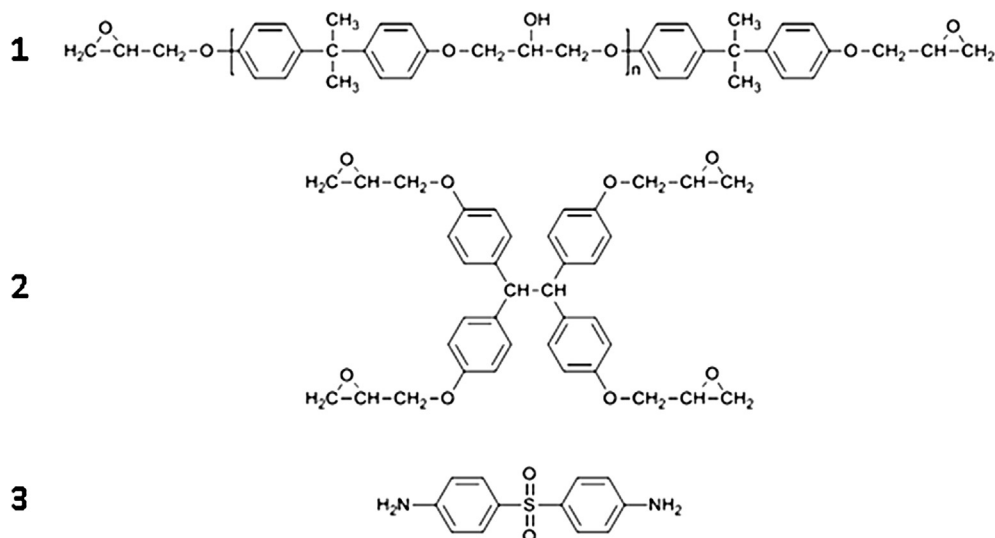


Fig. 1. Molecular structures of (1) EPON828 [ $n \sim 0.1$ ], (2) EPON1031, and (3) DDS.

density; higher crosslink density leads to higher  $T_g$  materials. As a polymer chemically degrades, the scission of chemical bonds will reduce the crosslink density and leads to an anticipated reduction in  $T_g$ . Since  $T_g$  is a function of the crosslink density, it is believed that  $T_g$  can be used to monitor thermal degradation.

## 2. Experimental

### 2.1. Materials

The constituent materials of the epoxy system were EPON828, EPON1031, and 4,4'-aminophenylsulfone (DDS). The molecular structures are shown in Fig. 1. EPON828 and EPON1031 were purchased from E. V. Roberts. DDS was purchased from Sigma–Aldrich. The epoxy system was prepared by mixing a 50–50 wt% mixture of EPON828 and EPON1031. The DDS curative is added to the EPON828–1031 mixture in a 1:1 equivalent of glycidyl to amine. The calculated amount of DDS was 31 pbw to 100 pbw of EPON828–1031. Samples were pre-cured at a temperature of 120 °C for 90 min followed by a thermal ramp of 1 °C/min to 230 °C and a 30 min post-cure at 230 °C. The prescribed cure schedule was previously shown to result in complete cure of the resin as assessed by differential scanning calorimetry and dynamic mechanical analysis [10].

### 2.2. Thermal aging

Rectangular samples with dimensions of 30 mm × 5 mm × 1.5 mm were aged isothermally in air at 210, 220, 230, 240, 250 °C in laboratory convection ovens with a temperature uniformity rating of ±2 °C. The temperatures were selected to provide significant degradation of the network on the order of days up to one year. The temperatures are above the continuous temperature rating of commercial high temperature epoxies which tend to be in the range of 150–200 °C. Samples were randomly taken from different locations in the aging oven to minimize error from oven temperature gradients. The relative humidity was 5% referenced to 25 °C. The initial  $T_g$  of the network is 245 °C. The majority of the aging temperatures initially are below the  $T_g$  of the network meaning that most

samples are initially in a vitrified state while some samples are aged at temperatures near the  $T_g$  and will be softer (see Fig. 3). A reduction in  $T_g$  will cause some samples to transition from a vitrified state to a rubbery state as the  $T_g$  is reduced. Vitrified epoxy cured networks aged in air where there is the potential for thermal oxidative degradation quickly become oxygen diffusion limited at the network–air interface [17]. The rate of thermal oxidation slows with depth due to a lack of oxygen in the interior of the sample. Diffusion is significantly retarded limiting thermal oxidation to a thin diffusion layer at the network surface. Diffusion is less hindered in a rubbery network due to the translational mobility of network segments allowing small molecules to diffuse more freely and leading to a thicker diffusion layer for thermal oxidative degradation. A reduction in the  $T_g$  of a network thermally aged near its glass transition temperature may have a profound effect on the rate of degradation and the degradation mechanism: pyrolytic in vitrified networks and a combination of pyrolytic and thermal oxidative in rubbery networks.

The rigidity of the DDS constituent imparts a high  $T_g$  to the network which will cause thermal oxidation of the network to be diffusion limited. Yet, to probe the role of diffusion limited oxidation, the  $T_g$  reduction of samples aged in inert argon was compared to the  $T_g$  reduction of samples aged in air. Samples aged in air are susceptible to diffusion limited oxidative degradation unlike samples aged in argon. Fig. 2 shows the absolute  $T_g$  reduction for two sets of samples aged at 240 °C in an air and argon environment. The  $T_g$  reduction at short time is not sensitive to the environment shown by the overlay of the  $T_g$  aged in air and in argon. The  $T_g$  of the network drops 45 °C (40 °C below the environment temperature) such that the network is thoroughly in a rubbery state. At long time, the  $T_g$  reduction is greater for the sample aged in air. The data shows that  $T_g$  reduction at short time is the result of non-oxidative pyrolytic degradation. Diffusion limited oxidative degradation contributes to the absolute reduction in  $T_g$  at long time in addition to continued pyrolytic degradation [18]. The contribution of oxidative degradation at long time may result from an increase in oxygen as the network transitions clearly to a rubber state. The  $T_g$  reduction comparison between the network aged in air and in argon implies that samples aged in air become heterogeneous at long time with pyrolytic degradation in the bulk of the sample and

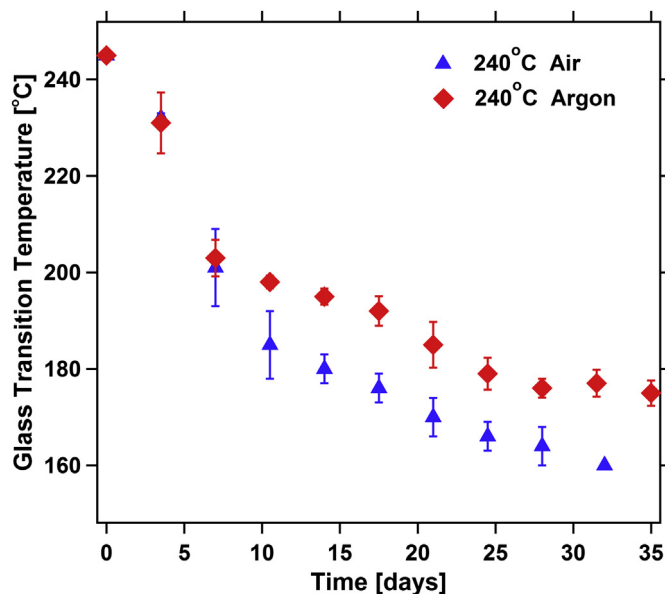


Fig. 2. Glass transition temperature as measured by DMA of aged EPON828–1031/DDS at a temperature of 240 °C in air and in inert argon.

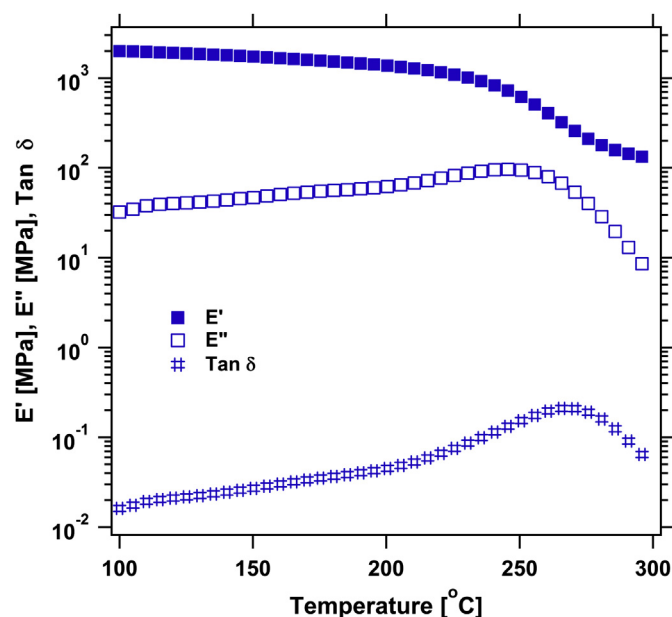


Fig. 3. DMA measurement of the storage and loss moduli and  $\tan \delta$  versus temperature of EPON828–1031/DDS by single cantilever beam.

oxidative degradation accompanying pyrolytic degradation at the surface. The  $T_g$  measurement of samples aged in air at long time is therefore an average over the cross section of the sample.

### 2.3. DMA

Dynamic mechanical measurements were performed using single cantilever beam geometry on a TA Instruments DMA Q800. The low strain in-phase and out-of-phase deformation response was measured when applying an oscillatory force with a controlled deformation amplitude of 20  $\mu\text{m}$  at a frequency of 1 Hz, and the resulting storage and loss moduli were calculated. The temperature was ramped at 3  $^{\circ}\text{C}/\text{min}$  over a temperature range spanning the glass to rubber transition. Fig. 3 shows the storage and loss moduli and  $\tan \delta$  for EPON828-1031/DDS cured network before thermal aging. The loss modulus peak occurs at a temperature of 245  $^{\circ}\text{C}$  which is a measure of  $T_g$ . The peak in  $\tan \delta$  is considered a second measurement of  $T_g$  and occurs at a slightly higher temperature than the peak in the loss modulus. All measurements of the  $T_g$  of samples were performed by DMA measurement and reference the peak temperature of the loss modulus.

### 2.4. Degradation model

The extent of  $T_g$  reduction is modeled with a degradation kinetics rate expression of the form

$$\frac{dp}{dt} = k(T)f(p) \quad (2)$$

where  $p$  is the extent of degradation,  $t$  is time,  $k(T)$  is a temperature sensitive degradation rate constant and  $f(p)$  is an extent of degradation function that depends on the reaction mechanism. Based on the comparison of the  $T_g$  reduction of samples aged in air and in argon, network degradation appears dominated by pyrolytic degradation with some oxidative degradation contribution at long time. Gas evolution degradation studies have shown initial non-oxidative degradation of an epoxy network to be dominated by

dehydration becoming significant at temperatures above 200  $^{\circ}\text{C}$  in phenol based epoxy cured networks [19,20]. Dehydration does not result in scission of the chemical network but the formation of an enamine in the network. In the EPON828-1031/DDS system, the enamine is adjacent to a phenolic ether bond originating from the EPON828 and EPON1031 resins. Following dehydration, the phenolic ether bond is preferentially broken due to its lower thermal stability from proximity to the enamine following dehydration [19]. The preferential chain scission of the phenolic ether bond is confirmed by phenol compounds as the major degradation species of phenol based epoxy cured network degradation products [19,21].

The rate of dehydration is expected to be steady in time since the concentration of network alcohols formed during the epoxy-amine network forming reaction is large at the onset of thermal aging. The enamine concentration is near zero at the onset of thermal aging and would only be present if dehydration occurred during network formation. Since bond scission depends on the enamine concentration, the initial rate of bond scission is low at temperatures sufficient to promote dehydration. As the enamine concentration increases in time from dehydration, the rate of bond scission of the phenolic ether bond will accelerate giving a sigmoidal character to the extent of network bond scission and  $T_g$  reduction. The sigmoidal shape is due to an induction period where network bond scission is initially slow followed by a rapid increase in rate as the concentration of the enamine increases and a slow tail as the concentration of remaining phenol ether bonds decreases. As is discussed later in Section 3, the  $T_g$  reduction at higher temperatures appears to be affected by additional higher temperature activated pyrolysis. Therefore, pyrolysis is more complex than the dehydration-bond scission mechanism described above as the aging temperature is increased. To avoid the complicated nature of pyrolytic degradation and enable modeling of the  $T_g$  reduction with step changes in temperature, an empirical form of  $f(p)$  that has been shown to model reaction mechanisms with an apparent induction period well is  $(a + p^m)(1 - p)^n$  [22]. Exponents  $m$  and  $n$  are order parameters that model the degradation mechanism, and the constant  $a$  accounts for an initial degradation rate at  $t = 0$  that may be nonzero. An Arrhenius relation is assumed to quantify the temperature dependence of the degradation rate constant,  $r_d$ . The overall rate expression for the extent of degradation,  $p_d$ , is written as

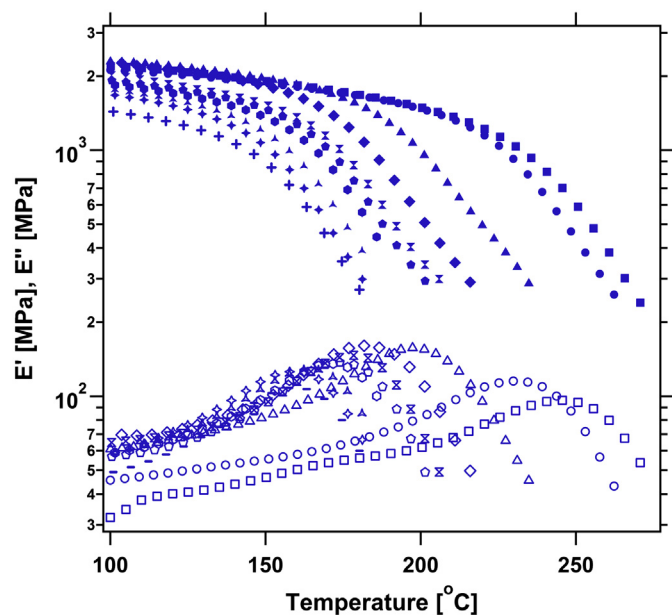


Fig. 4. Storage and loss modulus of EPON828-1031/DDS thermal aged at a temperature of 240  $^{\circ}\text{C}$  in air for 0 (square), 3.5 (circle), 7 (triangle), 10.5 (diamond), 14 (hourglass), 17.5 (pentagon), 21 (hexagon), 24.5 (tristar), 28 (quadstar), 31.5 (plus/minus) days.

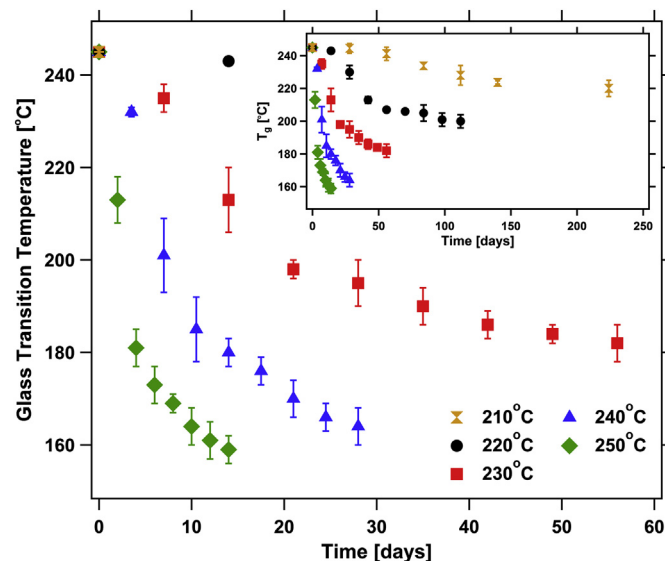


Fig. 5. Glass transition temperature as measured by DMA of aged EPON828-1031/DDS in air at temperatures of 210, 220, 230, 240, and 250  $^{\circ}\text{C}$ .



$$r_d = \frac{dp_d}{dt} = k_{0,d} e^{-E_a/RT} (a + p_d^m)(1 - p_d)^n. \quad (3)$$

### 3. Results

Long time thermally aged  $T_g$  reduction experiments were performed to assess degradation in terms of an extent of  $T_g$  reduction. The  $T_g$  of isothermally aged epoxy samples was measured by DMA. DMA measurement proved to be the best measurement technique based on sensitivity and consistency. The measurement is extremely sensitive to changes in stiffness enabling high fidelity measurements and  $T_g$  to be determined within  $\pm 0.5$  °C.  $T_g$  measurement by differential scanning calorimetry (DSC) did not yield a reliable measurement. DSC suffered from a weak thermal signature due to the high crosslink density of the network which made for inconsistent measurement of the  $T_g$ . Thermal mechanical analysis is an alternative measurement method of  $T_g$  but was not pursued. Measurements were consistent between multiple measurements of a single sample and between samples in a set which resulted in small error limits in the  $T_g$  measurement. The  $T_g$  is recorded as the peak in the loss modulus and averaged over three to five sample measurements of equivalent aging time. The standard error is calculated from the spread of the  $T_g$  measurements of a set of samples of the same age time and temperature. As the network is thermally aged in air, the peak in the loss modulus shifts to lower temperature, evidence of a reduction in  $T_g$ , Fig. 4. The reduction in  $T_g$  is caused by the scission of network bonds that reduce the crosslink density [23]. The reduction of the magnitude of the storage modulus at temperatures below  $T_g$  supports a reduction in crosslink density due to network bond scission since the magnitude of the storage modulus is linearly proportional to the crosslink density.

The  $T_g$  of thermally aged samples is plotted versus aging time in Fig. 5. The  $T_g$  rapidly declines at short time witnessed at all five aging temperatures. At longer aging time, the reduction in  $T_g$  appears to slow and transition to a more gradual decline. The reduction in  $T_g$  is greater at higher temperatures. Based on the earlier conclusion in Section 2.2 that network degradation proceeds via non-oxidative pyrolytic bond scission, the greater reduction in

$T_g$  at higher temperatures is attributed to a greater extent of bond scission of more thermally stable bonds that is accelerated at higher temperatures leading to a greater extent of bond breakage in addition to those that dominate at lower temperatures. Network bonds have differing thermal stabilities which affects the probability that a bond will break at a set temperature. A study of the degradation of another epoxy resin cured with DDS followed by gas evolution analysis during epoxy decomposition identified three partially overlapping degradation regimes where the scission of chemical bonds results in different evolved gases [20]. The first degradation regime is dominated by the evolution of water from the dehydration of secondary alcohols forming an enamine which reduces the stability of the ether bond adjacent to the enamine leading to thermal bond scission. The second and third degradation regimes involve more thermally stable bonds and are present to a greater extent at higher temperatures. These degradation pathways lead to a greater extent of bond scission. It is conceivable that degradation pathways of the second and third degradation regimes will be more active at a temperature of 250 °C than at the lower temperature of 210 °C. The consequence of these other degradation pathways on the  $T_g$  is a progressive lowering of the long time  $T_g$  reduction plateau. The differing extremes in  $T_g$  reduction make a time–temperature superposition of the absolute  $T_g$  reduction not possible.

How to account for the added bond scission is not straight forward. It is apparent that the absolute  $T_g$  reduction cannot be used to elicit the effect of temperature on the acceleration of  $T_g$  reduction. It is also apparent that the  $T_g$  reduction plateau at long time is temperature sensitive. In order to account for the contribution of secondary higher temperature accelerated degradation pathways and assess degradation due to dehydration which dominates initial network degradation at low temperature,  $T_g$  reduction is compared between temperatures through the extent of  $T_g$  reduction,  $p_{T_g}$ . This type of analysis is also used in isothermal TGA measurements to account for differences in the long time absolute weight loss of samples aged at different temperature. Polymers aged at high temperature approach long time weight loss that is greater (higher amount of weight loss) than materials aged at a lower temperature. The greater absolute weight loss at higher temperature is a function

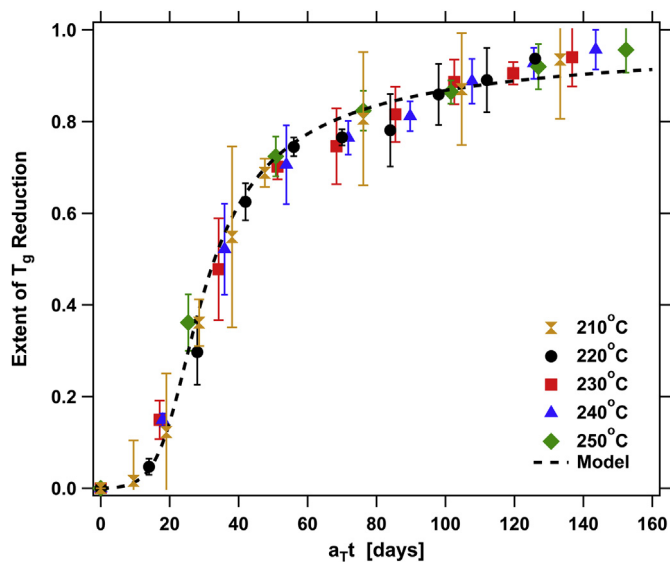


Fig. 6. Time–temperature superposition at a reference temperature of 220 °C of the extent of  $T_g$  reduction [Eq. (4)] of aged EPON828-1031/DDS in air as measured by DMA at temperatures of 210, 220, 230, 240, 250 °C. Dashed line is the model prediction of Eq. (5) at a reference temperature of 220 °C.

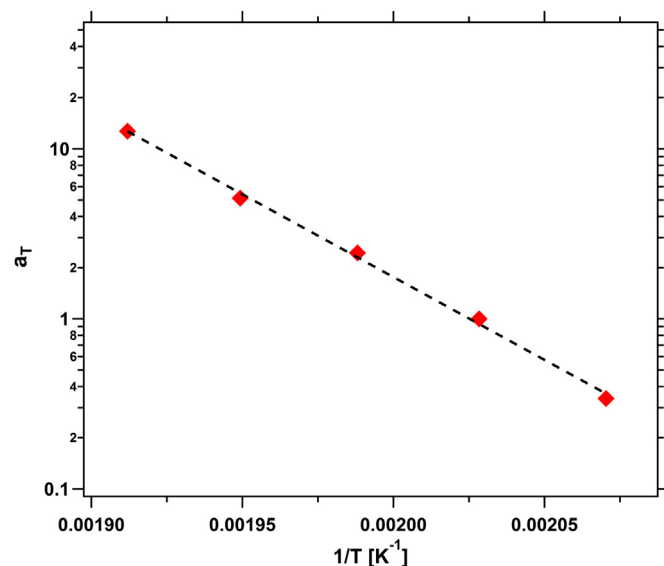


Fig. 7. Arrhenius plot of the temperature shift factors ( $T_{ref} = 220$  °C) versus the inverse temperature from time–temperature superposition of the extent of  $T_g$  reduction of EPON828-1031/DDS.

of the temperature supplying enough thermal energy to activate higher temperature degradation pathways and to volatilize higher molecular weight degradation products.

The extent of  $T_g$  reduction is defined as

$$p_{T_g} = \frac{(T_{g,i} - T_{g,a})}{(T_{g,i} - T_{g,f})} \quad (4)$$

where  $T_{g,i}$  is the initial  $T_g$  of the network,  $T_{g,f}$  is the final  $T_g$  of the network reached at long time, and  $T_{g,a}$  is the real time  $T_g$  of the aged network [9,18,24]. The extent of  $T_g$  reduction attempts to account for the contribution of secondary degradation by normalizing the real time  $T_g$  reduction by a long time  $T_g$  reduction based on  $T_{g,f}$ . Notice that the long time data in Fig. 5 have not reached a well-defined lower plateau although the initial drop in  $T_g$  is captured, and the reduction in  $T_g$  is approaching a more gradual decline. Therefore,  $T_{g,f}$  is an adjustable parameter that enables vertical adjustment of the extent of  $T_g$  reduction to enable a time–temperature superposition.

Fig. 6 shows the best fit superposition of the extent of  $T_g$  reduction versus shifted time,  $a_T t$ , at a reference temperature of 220 °C. Of interest is whether the temperature dependence of the  $T_g$  reduction can be well described by an Arrhenius relation. An Arrhenius plot of the temperature shift factors,  $a_T$ , versus  $1/T$  gives a straight line supporting an Arrhenius relation between  $p_{T_g}$  and  $T$  (Fig. 7). The slope of the linear best fit gives an activation energy of  $187 \pm 6$  kJ/mol. Utilizing the derived activation energy, the extent of  $T_g$  reduction was fit by an autocatalytic degradation model (Eq. (5)) using a non-linear least squares regression analysis. The fit shown in Fig. 6 is able to capture the decline in  $T_g$  reasonably well.

$$\frac{dp_{T_g}}{dt} = k_{0,T_g} e^{-E_a/RT} (0.001 + p_{T_g}^{0.96}) (1 - p_{T_g})^{2.5}$$

$$E_a = 187 \text{ kJ/mol} \quad (5)$$

$$k_{0,T_g} = 9.3 \times 10^{15} \text{ min}^{-1}$$

#### 4. Discussion

EPON828-1031/DDS shows a reduction in  $T_g$  as the polymer was aged isothermally in air at elevated temperature. Comparison of the  $T_g$  reduction of samples aged in air to samples aged in inert argon shows that degradation is dominated by non-oxidative pyrolytic bond scission. The time scale of the reduction is temperature dependent such that an increase in temperature caused a more rapid reduction in  $T_g$  at short time. The absolute reduction in  $T_g$  is converted to an extent of reduction and a time–temperature superposition is constructed. The temperature shift factors are shown to display an Arrhenius temperature dependence. The Arrhenius behavior supports  $T_g$  reduction as directly impacted by thermal bond scission and as a means of quantifying thermal degradation. The activation energy determined from an Arrhenius plot is found to be similar to the activation energy determined previously for EPON828-1031/DDS from adhesion degradation experiments,  $184 \pm 5$  kJ/mol, and higher temperature gravimetric weight loss measurements,  $180 \pm 4$  kJ/mol [10]. The similarity implies that  $T_g$  reduction is controlled by the same intrinsic degradation process over the studied temperatures and that  $T_g$  can be used as an observable of polymer degradation for lifetime estimates.

The reduction in  $T_g$  is shown to have a sigmoidal character due to an induction period where the rate of  $T_g$  reduction is initially slow but accelerates in time with greater  $T_g$  reduction. The initial chemical process of non-oxidative pyrolytic degradation is dehydration and thermal scission of network bonds weakened by

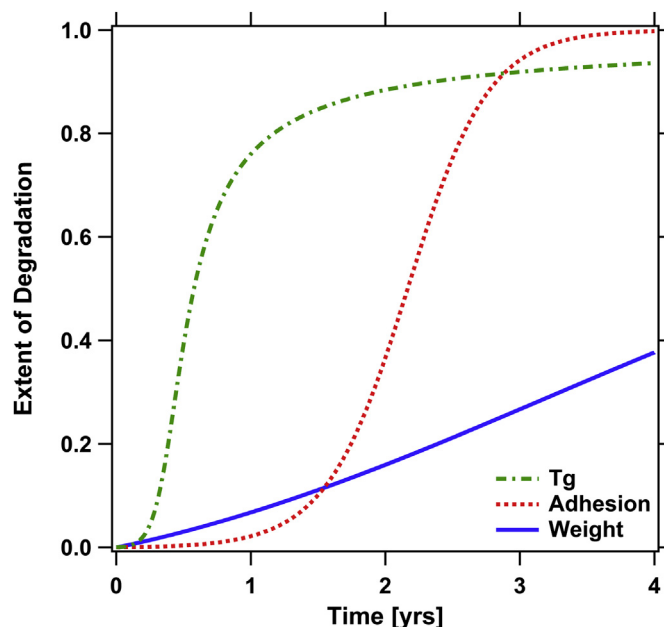


Fig. 8. Predictions of the autocatalytic degradation model as determined from  $T_g$  reduction measurements compared to model predictions of the extent of degradation from adhesion and weight measurements for EPON828-1031/DDS at an isothermal temperature of 200 °C [10].

dehydration leading to the formation of a phenol and a quinoline in phenol ether based epoxy resins (e.g., EPON828 and EPON1031). [19,21] Dehydration is expected to be steady in time since the concentration of network alcohols formed during the epoxy-amine network forming reaction is large at the onset of thermal aging. An enamine is formed as a result of dehydration which weakens the phenolic ether network bond adjacent to the enamine. Network bond scission preferentially occurs at the phenolic ether bond. The enamine concentration is near zero at the onset of thermal aging and would only be present if dehydration occurred during formation of the network. Since bond scission depends on the enamine concentration, the rate of bond scission is initially low. As the enamine concentration increases in time from dehydration, the rate of bond scission of the phenolic ether bond will accelerate giving a sigmoidal character to  $T_g$  reduction with time.

The absolute reduction in  $T_g$  is shown to be more severe at higher aging temperatures. A case was made for the existence of several degradation pathways that contribute to degradation and result in a greater reduction in  $T_g$  with temperature. Non-oxidative pyrolytic degradation of amine cured epoxy networks has been shown to be characterized by three partially overlapping degradation regimes that accelerate at higher temperature [20]. It is argued that higher temperature activated degradation pathways will be present at higher aging temperatures than at lower aging temperatures. The consequence of these added degradation pathways is a more extreme reduction in  $T_g$  at higher temperatures due to greater breakdown of the network and a progressive lowering of the long time  $T_g$  reduction plateau. To account for the effect of higher temperature degradation on the rate of  $T_g$  reduction and the final  $T_g$  at long time, the absolute  $T_g$  reduction is converted into an extent of  $T_g$  reduction based on the initial and final  $T_g$  values as a means of comparing the rate of  $T_g$  reduction in terms of extent. This is a means of taking into account all the chain scission events that contribute to the absolute  $T_g$  reduction. When the absolute  $T_g$  reduction is taken into account in terms of an extent of  $T_g$  reduction, the extent of  $T_g$  reduction displays an Arrhenius temperature

dependence and an activation energy is extracted that agrees well with previous measurements.

The Arrhenius scaling of the extent of  $T_g$  reduction rather than the absolute  $T_g$  reduction was not appreciated in a recent paper that attempted to extract degradation activation energies based on absolute  $T_g$  reduction [14]. The study only captured an initial drop in  $T_g$  and did not capture a transition to a slower more steady decline in  $T_g$  at long time or discern whether the  $T_g$  was approaching a long time  $T_{g,f}$ . The study may not have been conducted to long enough time. An activation energy was extracted based on the absolute  $T_g$  reduction of the polymer which potentially leads to an incorrect activation energy. The activation energy was not compared to other observable measurements of degradation for the material. Assuming the material is also prone to a long time  $T_{g,f}$  that is lowered with higher aging temperature, the derived activation energy based on the absolute  $T_g$  reduction will be larger than the activation energy that would be determined based on the extent of reduction giving the appearance of a more thermally stable material and a longer estimated lifetime. Aging studies must be conducted to long enough time to discern the full character of the observable being studied and its dependence on material degradation. In addition, activation energies should be determined from a non-dimensional extent of degradation of the observable studied.

Fig. 8 shows a comparison of the  $T_g$  reduction model to previous models established from adhesion and weight degradation measurements for EPON828-1031/DDS. The models show  $T_g$  reduction to be more sensitive to degradation at short time than adhesion and weight. The chemical mechanism of degradation is the scission of chemical bonds that make up the internal network of the polymer. The reduction of the storage modulus which is proportional to the crosslink density supports thermal bond breakage and a reduction in the crosslink density as the network is thermally aged. As bonds are broken, the crosslink density of the network is reduced causing a reduction in  $T_g$ . Notice that the weight loss of the epoxy is more gradually reducing as gaseous degradation products are released with the breaking of chemical bonds.  $T_g$  and adhesion are initially little affected. The result shows that there is an induction period with observables such as  $T_g$  and adhesion. The induction period is the result of dehydration which does not lead to the scission of network bonds but does liberate water leading to weight loss. The thermal resistance of the network is lowered due to dehydration leading to an acceleration in thermal bond scission.  $T_g$  reduction proves to be more sensitive to network bond scission than adhesion. When the lifetime of the polymer is considered in a used environment, it is evident that lifetime assessments and failure analysis need to account for  $T_g$  reduction. (Note: The adhesion lifetime model in Fig. 8 shows the effect of thermal degradation on the glassy adhesion strength. As long as the  $T_g$  of the network remains above the temperature of the environment, the adhesion strength is expected to follow the extent of degradation of the glassy adhesion strength. As the  $T_g$  of the polymer approaches the environment temperature, a proximity effect of the  $T_g$  to the environment temperature will lead to a reduction in the adhesion strength due to transition of the polymer from a glassy state to a rubbery state.) [16].

## 5. Conclusion

The thermal degradation of an epoxy cured network is studied by  $T_g$  reduction measurements. The  $T_g$  is shown to decline as the polymer is aged at elevated temperature for long time in air and in inert argon. Thermal degradation of the network in air is dominated by non-oxidative pyrolysis of the network at short time. Oxidative degradation contributes to  $T_g$  reduction at long time resulting in a greater absolute  $T_g$  reduction in air than in argon. The

results for this epoxy network are most applicable to predicting lifetime when thermal degradation is pyrolytic in nature. At lower temperatures in air, oxidative degradation may supersede pyrolytic degradation. Oxidation reactions have lower activation energies [25]. However, the network will be in a vitrified state at lower temperatures which will quickly cause oxidative degradation to be diffusion limited. Therefore, non-oxidative pyrolytic degradation is likely to continue to dominate thermal degradation at lower temperatures as long as samples are much thicker than the oxidative diffusion layer.

The extent of  $T_g$  reduction has an Arrhenius temperature dependence with a constant activation energy over the temperatures studied. The degradation activation energy from the extent of  $T_g$  reduction agrees well with degradation activation energies derived from other property measurements for the same polymer. The agreement of the activation energy with past results shows that  $T_g$  reduction as a measure of thermal degradation depends on the extent of  $T_g$  reduction and can be used as an observable for lifetime estimates. In addition, the time scale of  $T_g$  reduction is compared to previous property measurements to show the difference in sensitivity of observable material properties on degradation. The  $T_g$  of the polymer is shown to be more sensitive to degradation than other property measurements leading to a rapid rise in the extent of degradation at shorter time for a similar temperature. The result emphasizes the importance of proper selection of an observable property measurement when performing aging experiments intended for estimating lifetimes of materials.

## Acknowledgment

The author thanks Joanneta Bruhn for material sample preparation, thermal aging of samples, and DMA testing. The author also thanks Mat Celina for helpful comments with regard to preparation of the manuscript. Sandia is a multiprogram laboratory operated by Sandia Corporation, a Lockheed Martin Company, for the United States Department of Energy under contract DE-AC04-94AL85000.

## References

- [1] Celina M, Gillen KT, Assink RA. Accelerated aging and lifetime prediction: review of non-Arrhenius behaviour due to two competing processes. *Polymer Degradation and Stability* 2005;90:395–404.
- [2] Flynn JH. Degradation kinetics applied to lifetime predictions of polymers. *Society of Plastics Engineers, Inc.*; 1980. p. 675–7.
- [3] Flynn JH. Lifetime prediction for polymers from thermal analytical experiments – problems and how to deal with some of them. *Thermochimica Acta* 1988;134:115–20.
- [4] Flynn JH. A critique of lifetime prediction of polymers by thermal analysis. *Journal of Thermal Analysis* 1995;44:499–512.
- [5] Freeman ES, Carroll B. The application of thermoanalytical techniques to reaction kinetics: the thermogravimetric evaluation of the kinetics of the decomposition of calcium oxalate monohydrate. *The Journal of Physical Chemistry* 1958;62:394–7.
- [6] Bernstein R, Gillen KT. Nylon 6.6 accelerating aging studies: II. Long-term thermal-oxidative and hydrolysis results. *Polymer Degradation and Stability* 2010;95:1471–9.
- [7] Gillen KT, Bernstein R, Derzon DK. Evidence of non-Arrhenius behaviour from laboratory aging and 24-year field aging of polychloroprene rubber materials. *Polymer Degradation and Stability* 2005;87:57–67.
- [8] Gugumus F. Effect of temperature on the lifetime of stabilized and unstabilized PP films. *Polymer Degradation and Stability* 1999;63:41–52.
- [9] Nam J-D, Seferis JC. Generalized composite degradation kinetics for polymeric systems under isothermal and nonisothermal conditions. *Journal of Polymer Science Part B: Polymer Physics* 1992;30:455–63.
- [10] Anderson BJ. Thermal stability of high temperature epoxy adhesives by thermogravimetric and adhesive strength measurements. *Polymer Degradation and Stability* 2011;96:1874–81.
- [11] Gillen KT, Keenan MR, Wise J. New method for predicting lifetime of seals from compression-stress relaxation experiments. *Die Angewandte Makromolekulare Chemie* 1998;261–262:83–92.
- [12] Tiganis BE, Burn LS, Davis P, Hill AJ. Thermal degradation of acrylonitrile-butadiene-styrene (ABS) blends. *Polymer Degradation and Stability* 2002;76:425–34.

- [13] Petrie EM. Handbook of adhesives and sealants. New York: McGraw-Hill; 2007.
- [14] Polanský R, Mentlík V, Prosr P, Susír J. Influence of thermal treatment on the glass transition temperature of thermosetting epoxy laminate. *Polymer Testing* 2009;28:428–36.
- [15] Wondraczek K, Adams J, Fuhrmann J. Effect of thermal degradation on glass transition temperature of PMMA. WILEY-VCH Verlag; 2004. p. 1858–62.
- [16] Cassidy PE, Johnson JM, Locke CE. Relationship of glass transition temperature to adhesive strength. *Journal of Adhesion* 1972;4:183–91.
- [17] Le Huy HM, Bellenger V, Paris M, Verdu J. Thermal oxidation of anhydride cured epoxies II – depth distribution of oxidation products. *Polymer Degradation and Stability* 1992;35:171–9.
- [18] Salla JM, Morancho JM, Ramis X, Cadenato A. Isothermal degradation and thermooxidative degradation of an epoxy powder coating. *Journal of Thermal Analysis and Calorimetry* 2005;80:163–9.
- [19] Leisegang EC, Stephen AM, Paterson-Jones JC. The thermal degradation in vacuo of an amine-cured epoxide resin. *Journal of Applied Polymer Science* 1970;14:1961–81.
- [20] Levchik SV, Camino G, Luda MP, Costa L, Costes B, Henry Y, et al. Mechanistic study of thermal behaviour and combustion performance of epoxy resins. II. TGDDM/DDS system. *Polymer Degradation and Stability* 1995;48:359–70.
- [21] Lee L-H. Mechanisms of thermal degradation of phenolic condensation polymers. II. Thermal stability and degradation schemes of epoxy resins. *Journal of Polymer Science Part A: General Papers* 1965;3:859–82.
- [22] Hadad DK. Physical and chemical characterization of epoxy resins. In: May CA, editor. *Epoxy resins*. 2nd ed. New York: Marcel Dekker, Inc; 1988. p. 1089–172.
- [23] Gillham JK. Formation and properties of thermosetting and high  $T_g$  systems. In: Güven O, editor. *Crosslinking and scission in polymers*. Netherlands: Springer; 1990. p. 171–98.
- [24] Patel RD, Patel RG, Patel VS. Kinetics of thermal degradation of cured epoxy resins based on triglycidyl-p-aminophenol. *Thermochimica Acta* 1988;128:149–56.
- [25] Celina MC, Dayile AR, Quintana A. A perspective on the inherent oxidation sensitivity of epoxy materials. *Polymer* 2013;54:3290–6.